Is the Al-Pd-Mn icosahedral phase centrosymmetrical?

1994 J. Phys.: Condens. Matter 6 363

(http://iopscience.iop.org/0953-8984/6/2/008)

J. Phys.: Condens. Matter 6 (1994) 363–373. Printed in the UK

Is the Al–Pd–Mn icosahedral phase centrosymmetrical?

M de Boissieu†‡, P Stephens†, M Boudard‡§ and C Janot§‖

† Department of Physics, State University of New York at Stony Brook, NY 11794, USA

‡ Laboratoire de Thermodynamique et Physico-Chimie Métallurgiques, Ecole Nationale Supérieure d'Electrochimie et d'Electrométallurgie de Grenoble (Unité associée au CNRS 29), BP 75, 38 402 St Martin d'Hères Cédex, France

§ Institut Laue–Langevin, BP 156, 3042 Grenoble Cédex 9, France

‖ Laboratoire de Cristallographie, CNRS, BP 166, 38042 Grenoble Cédex, France

Received 3 August 1993, in final form 24 September 1993

Abstract. The possible non-centric character of the icosahedral Al–Pd–Mn phase has been checked by measuring Bijvoet pairs above the Pd K edge on a single grain. The integrated intensity of HKL and $-H-K-L$ reflections is found to be identical within the experimental errors. The computed intensity variation for 45° phase differences are computed to be much larger than the observed values. This indicates that the icosahedral phase is centrosymmetrical or presents phases very close to 0 or π.

1. Introduction

The atomic structure of quasi-crystals is now mostly understood by means of high-dimensional crystallography [1–5]. In this scheme the quasi-periodic structure is given a periodic image in a higher-dimensional space. This periodic space decomposes into two subspaces: E_{par}, the physical space, and E_{perp}, the perpendicular space. For icosahedral quasi-crystals the periodic space needs to have dimensions of at least 6. The periodic lattice is decorated by atomic surfaces, which typically extend in E_{perp}. The corresponding 3D quasi-periodic structure is then obtained as a cut along E_{par} through the decorated periodic lattice. A simple illustration of a 2D periodic image which generates a cut 1D quasi-periodic structure is given in figure 1(a).

The route from diffraction data to the atomic structure of a quasi-crystal is similar to what is done in 3D crystallography [6, 7]. The first step is the determination of Bravais lattice, the point group and the space group of the diffraction pattern, with the proper basis vectors. In a second step, a Patterson analysis generally allows one to approximate the atomic surfaces. Finally one has to refine precisely the six-dimensional shape of the different atomic surfaces.

Most of the attention in the solution of quasi-crystal structures has been given to the problems of determining and refining the shapes of the atomic surfaces, through a variety of specific experimental and theoretical approaches [8–15]. In contrast, there has been relatively little work which directly addressed the determination of the crystallographic point group, and in particular the presence or absence of inversion symmetry.

As in conventional crystallography, the experimental determination of inversion symmetry from diffraction data is complicated by the fact that the observed intensities $I(Q)$ derive from the absolute square of the atomic structure factor $f(Q)$, so that $I(Q) = I(-Q)$, even if $f(Q) = f^*(-Q)$ is not equal to $f(-Q)$. Patterson analyses on icosahedral Al–Mn–Si [6, 9, 10], Al–Li–Cu [11], Al–Cu–Fe [16], and Al–Pd–Mn [17] show density correlations

0953-8984/94/020363+11$07.50

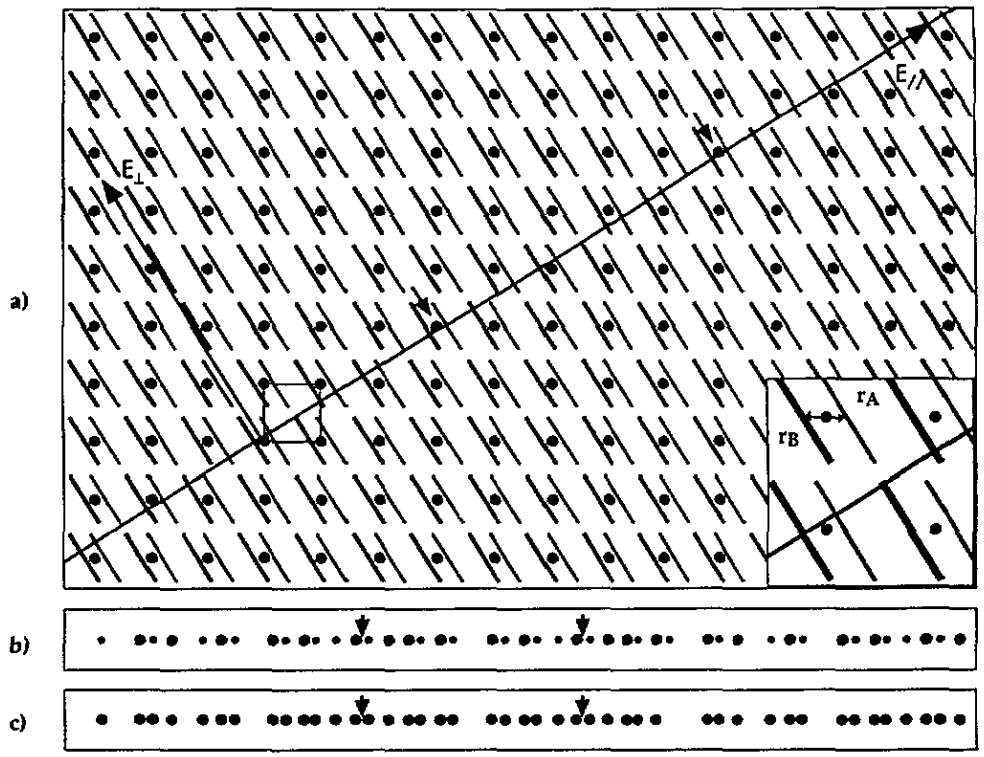

Figure 1. Example of a 1D quasi-periodic structure which is not centrosymmetrical. (*a*) The periodic 2D image of the 1D structure. The square lattice is decorated with two segment lines ('atomic surfaces') located at r_A and $r_B = -r_A$ in the square lattice. They have same length but different thicknesses to represent different chemical species. (*b*) The corresponding 1D structure. The two different atoms corresponding to the different chemical species are represented by different dot sizes. (*c*) The structure obtained when the two segment lines of (*a*) correspond to the same chemical species. Local environments with centrosymmetrical character are shown by an arrow.

only on special point of the 6D cube, suggesting centrosymmetric structures. The only density solution for such a Patterson function is one in which the structure is centric as long as the positions of atomic surfaces are concerned. However, their shape might have only 235 symmetry, leading to a non-centric space group [16, 18]. Further refinements of atomic structures in these materials, including contrast variation by isotopic substitution, have been performed without any evidence for the absence of inversion symmetry. However, these experiments are not directly sensitive to the presence of an inversion centre; non-centric character would be manifest only by comparing the quality of fits for specific centric and acentric atomic structures.

Three recent papers have addressed the problem of inversion symmetry in quasi-crystals directly and they all find non-centrosymmetric structures. The first uses convergent-beam electron diffraction to reveal that decagonal Al–Ni–Fe has the non-centrosymmetric space group $P\bar{1}0m2$ [19]. The second and third apply multiple-beam dynamic diffraction to icosahedral Al–Cu–Fe [20] and icosahedral Al–Pd–Mn [21] and claim that there is no inversion symmetry, in contrast with the results of detailed structural refinements on the same materials, including isotopic [22] and isomorphic [17] contrast variation.

Starting with this background knowledge, we have chosen a different experimental technique which investigates inversion symmetry directly, namely the comparison of Bijvoet pairs. Near the x-ray absorption edge, the atomic scattering factor shows a substantial phase shift. If there is an acentric structure, the geometric structure factor is not purely real, and reflections Q and $-Q$ will have different intensities. In the present study, we apply this technique to icosahedral Al–Pd–Mn at the Pd edge.

2. Centrosymmetry in quasi-crystals

To illustrate the nature of inversion symmetry in a non-periodic structure, we shall use a simple 1D quasi-crystalline model. The 2D image and the corresponding 1D quasi-periodic structure are presented in figures 1(a) and 1(b). Two different atomic surfaces have been positioned in the square unit cell at r_A and $r_B = -r_A$. As can be seen in the inset of figure 1(a), r_A and r_B have a component only along one of the edges of the unit cell. The two 'atomic surfaces' (segment lines) have the same length but different thicknesses to represent different atoms; this is what introduces the lack of centrosymmetry. The structure factor may be computed easily as

$$F(q) = G(q_{\text{perp}})[b_A \exp(iq \cdot r_A) + b_B \exp(iq \cdot r_B)] \tag{1}$$

where q is a reciprocal lattice vector with indices n_1 and n_2, $G(q_{\text{perp}})$ is the Fourier transform of the segment line, and b_A and b_B are the scattering lengths of atoms A and B, respectively. If $b_A = b_B$, the structure factor is a real quantity, but in general it will be a complex number.

What is the corresponding 1D structure like? In particular, how does the presence or absence of centrosymmetry show up? This is illustrated in figure 1(b), which is the result of the physical cut through the decorated periodic lattice. The two different atoms A and B are indicated by small and large dots corresponding to thin and thick atomic surfaces. Had the two chemical species been identical, the structure would have been centrosymmetrical. Let us first consider this case which is represented in figure 1(c). If the cut goes through one lattice site, then this point will be the *unique* centre of symmetry of the 1D structure. Around this point, for each atom located at r there is an equivalent atom located in $-r$, up to infinity. However, for a general position of the cut such as that represented in figure 1(a), there is no point of the 1D quasi-periodic structure that is a centre of symmetry. There are, however, sites of the periodic lattice arbitrarily close to the parallel space. Around such sites the structure has a local environment showing a centrosymmetrical arrangement up to some finite distance. Such sites are indicated by an arrow in figure 1(a)–1(c). We therefore see that a centrosymmetric quasi-crystal contains centrosymmetric domains of bounded size which can be shown to be quasi-periodically distributed.

Introducing the chemical decoration (atoms A and B) breaks centrosymmetry, as is now obvious in figure 1(b). Finally, note that $(0, n_2)$ reflections will necessarily have real structure factors. This is because the decoration of the square lattice involves only a horizontal component. Thus only reflections of the form (n_1, n_2) with $n_1 \neq 0$ will be complex numbers and have phases different from 0 or π.

The icosahedral case is a generalization of this simple 1D example. The two possible icosahedral point groups are 235 (Y) and $m\bar{3}\bar{5}$ (Y_I). Both have the same numbers of twofold, threefold and fivefold symmetry axes. The addition of a centre of symmetry in Y_I leads to new mirror planes. The possibility of an acentric icosahedral point group is illustrated in figure 2 (taken from [25]). Associated to each point group there are three possible Bravais

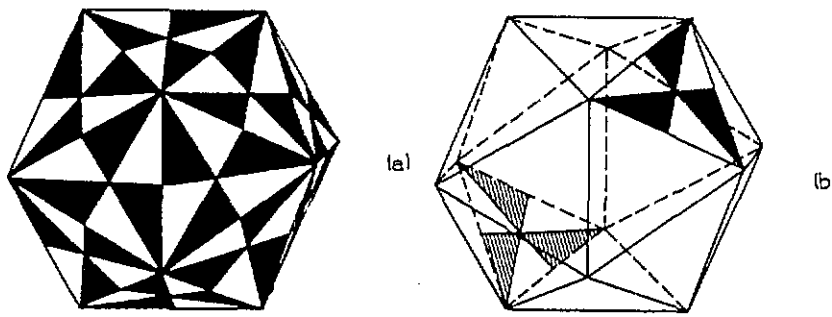

Figure 2. (*a*) Decorated icosahedron that is non-centrosymmetrical (from [25]). (*b*) Respective positions of black and white areas of (*a*) distributed in a non-centrosymmetrical way.

lattices: P, I, and F (derived from primitive cubic, body-centred cubic and face-centred cubic 6D lattices). Screw axes or glide planes added to these Bravais lattices lead to five additional non-symmorphic space groups, for a total of 11 [23–25].

The icosahedral Al–Pd–Mn phase exhibits an I-type reciprocal lattice [26,27], similar to that of icosahedral Al–Cu–Fe and corresponding to an F-type direct lattice. There are four possible space groups: two corresponding to Y and two corresponding to Y_I. The non-symmorphic space groups give rise to extinctions in the diffraction pattern. A careful examination of the x-ray and neutron diffraction pattern shows that all reflections are present, which rules out the existence of screw axes or glide planes. On the one hand the possible non-symmorphic space group corresponding to Y requires that all reflections with 6D indices [28] of the form $(l, n, l, -l, l, l)$, where l and n are integer and n is not a multiple of 5, should be absent [23–25]. Reflection 18/29 (see [28] for the indexation scheme) with 6D indices $(2, 4, 2, -2, 2, 2)$ which is of the required form is not extinguished in the case of the icosahedral Al–Pd–Mn phase and corresponds to one of the most intense reflections. On the other hand the possible non-symmorphic space group corresponding to Y_I requires that all reflections with 6D indices of the form $(n_1, n_2, n_3, n_4, n_2, -n_3)$ and such that $n_1 + n_4$ is not a multiple of 4 should be absent. Reflection 15/23 with 6D indices $(3, 3, 1, -1, 3, 1)$ which is of the required form has been measured without ambiguity. We are thus left with two possible symmorphic space groups: $F235$ or $Fm\bar{3}\bar{5}$.

In the icosahedral case, because we have symmorphic space groups, reflections on twofold, threefold and fivefold axes have real amplitudes even when considering the $F235$ space group, as point out by Cornier-Quiquandon *et al* [22]. Reflections in planes perpendicular to twofold axes (60 multiplicity in the $m\bar{3}\bar{5}$ point group) will also have real amplitudes. Only reflections in a general position (multiplicity, 120) can have phases different from 0 or π.

As an example, we can demonstrate that reflections on a twofold plane have a real amplitude as follows. To a point in the 6D cube with coordinates $\boldsymbol{R}_1 = (X_{\mathrm{par}}, Y_{\mathrm{par}}, Z_{\mathrm{par}}, X_{\mathrm{perp}}, Y_{\mathrm{perp}}, Z_{\mathrm{perp}})$ corresponds an equivalent point $\boldsymbol{R}_2 = (X_{\mathrm{par}}, -Y_{\mathrm{par}}, -Z_{\mathrm{par}}, X_{\mathrm{perp}}, -Y_{\mathrm{perp}}, -Z_{\mathrm{perp}})$ through a twofold rotation. Note that this would not be the case for a twofold screw axis. Reflections lying in a twofold plane may be expressed as $\boldsymbol{Q} = (0, QY_{\mathrm{par}}, QZ_{\mathrm{par}}, 0, QY_{\mathrm{perp}}, QZ_{\mathrm{perp}})$. When computing the structure factor $F(\boldsymbol{Q})$, the summation, which extends over all points in the 6D unit cell, may be expressed by regrouping terms related by a twofold rotation such as $\boldsymbol{R}_1$ and $\boldsymbol{R}_2$. The two scalar products $\boldsymbol{R}_1 \cdot \boldsymbol{Q}$ and $\boldsymbol{R}_2 \cdot \boldsymbol{Q}$ have the same magnitude and opposite signs, which leads to a real structure factor. This relation does not depend on the specific decoration of the

6D unit cell. We emphasize that this is an important consistency check for any experiment intended to observe the absence of centrosymmetry in a quasi-crystal.

3. Experimental details

X-ray Bijvoet pair measurement above an absorption edge is a well known tool to distinguish between centric and non-centric space groups [29]. When absorption and anomalous scattering effects take place, the atomic scattering form factor is written

$$f = f_0 + f' + \mathrm{i}f''$$

where f_0 is the usual atomic form factor, depending on the scattering wavevector, and f' and f'' depends on the x-ray wavelength but not on the scattering angle. f' is in phase with f_0, whereas f'' presents a $\frac{1}{2}\pi$ phase difference from f_0 (imaginary component). This implies a breakdown of the Friedel law for non-centric space groups. The situation is depicted in figure 3. F_A is the structure factor of the anomalous scattering element (Pd), and F_B that of the other atoms. If the phase difference is not equal to 0 or π, then $F(HKL)$ will be different from $F(-H-K-L)$.

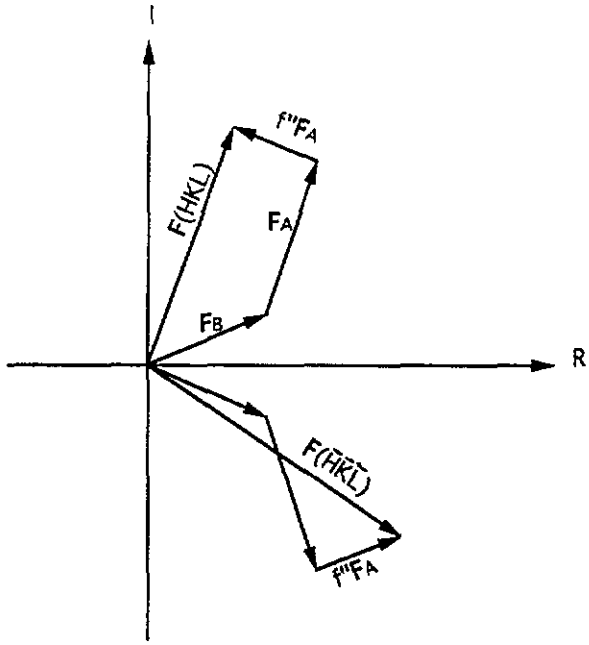

Figure 3. Illustration of the principle of Bijvoet pair measurements. F_A is the structure factor of the anomalous scatterer and F_B the structure factor of the remaining structure. When the anomalous effect takes place, f' and an f'' component have to be added to F_A. Since the phase difference F_A and f'' is always $\frac{1}{2}\pi$, $F(HKL)$ will have a different modulus from $F(-H-K-L)$.

The single-grain sample used for the measurements was extracted from the upper part of a Bridgman ingot. It is a 'perfect' icosahedral phase, with a composition $Al_{68.7}Pd_{21.6}Mn_{9.7}$

[30]. The sample was polished into a spherical shape, with a diameter of 160 μm and glued on the tip of a glass fibre. Data collection was carried out at the X3A2 beam line of the National Synchrotron Light Source, Brookhaven. A Si(220) double monochromator selected the incident energy of the unfocused beam. Integrated intensities were measured by the ω scan method. The mosaic spread of the sample was about 0.04° and consisted of two domains with 0.02° misorientation.

In order to enhance the effect, measurements were carried out just above the Pd K edge. The f'- and f''-values at the working energy of 24 390 eV, obtained from a Kramers–Kronig transform of the fluorescence spectrum measured through the Pd edge, are −5.17 and 3.55, respectively. Each reflection was centred before the measurement of integrated intensity. Because most of the reflections were very weak, especially at the high x-ray energy used, each measurement was taken at a rate of 4 s per point.

We measured 21 reflections in a general symmetry position over a large range of wavevectors. In order to check the reliability of the measurements, we also measured 20 reflections lying on a twofold plane in the same area of the reciprocal space. A subset of these reflections was measured on a second sample.

4. Discussion

The integrated intensities and the corresponding Poissonian deviations σ_{Poisson} and total standard deviations σ_{tot} are given in tables 1 and 2. Table 1 shows the results for those reflections lying on a general position (multiplicity 120) and table 2 presents results of the measurements for reflections lying on a symmetry position (multiplicity lower than 120) that must fulfil the condition $F(HKL) = F(-H-K-L)$. The total standard deviation is the combination of the standard deviation σ_{Poisson} corresponding to Poissonian statistics and a 'standard deviation' σ_{other} corresponding to other causes such as beam instability or a non-perfect spherical shape of the sample. An estimate of σ_{other} may be obtained from reflections lying on a symmetry position (table 2). We know that these reflections have real structure factors and this has indeed been observed within an accuracy of 3–5% for reflections with an intensity greater than 3000. For these reflections the Poissonian standard deviation is smaller than 0.02 and differences between the measurements allow us to evaluate σ_{other}. The standard deviation of the measured reflections may thus be written as $\sigma_{\text{tot}}^2 = \sigma_{\text{Poisson}}^2 + \sigma_{\text{other}}^2$ with $\sigma_{\text{other}} = 0.03I$, where I is the integrated intensity.

Table 1 shows that for those reflections lying on a general position there are no differences greater than three times the total standard deviation σ_{tot}, except for one reflection with indices 51/80. This reflection was measured again on another sample and did not show any difference between $F(HKL)$ and $F(-H-K-L)$ this time. The results in tables 1 and 2 are quite similar, which indicates that the structure is likely to be centrosymmetrical.

In order to interpret these data, it is necessary to compare them with a specific model of a deviation from centrosymmetry. This is estimated using a 'first-order' model extracted from x-ray and neutron single-crystal diffraction data [18]. The model is centrosymmetrical, but it may be used to evaluate the Pd and the Al–Mn contribution to the diffraction. An arbitrary phase difference of 45° between the two partial structure factors $F_{\text{Al-Mn}}$ and F_{Pd} is then introduced and the corresponding intensity variations are computed. In a real structure there is obviously no reason for this phase difference to be identical for all structure factors. However, in waiting for more detailed models, this allows a first evaluation of the expected intensity variation for a 45° phase difference. The results are shown in the last column of table 1. As can be seen, the intensity variation predicted for certain reflections is much

Table 1. Measured intensities of Bijvoet pairs of reflections in general symmetry positions (multiplicity 120). N, M, h, h', k, k', l and l' refer to the quasi-crystal indices as described in [28]. Q_{par} and Q_{perp} are the magnitudes of the physical and phason wavevectors, respectively; I_{norm} is the measured intensity, normalized to incident beam monitor; $\sigma_{Poisson}$ and σ_{tot} are the 'standard deviations' of I as explained in the text; DI/I is the measured difference between Bijvoet pairs, and $(DI/I)_{calc}$ is the calculated difference for a phase shift of 45° between Pd and Al–Mn, as described in the text.

N	M	Multiplicity	Q_{par}	Q_{perp}	h/h'	k/k'	l/l'	I_{norm}	$\sigma_{Poisson}$	σ_{tot}	DI/I	$(DI/I)_{calc.}$
51	80	120	4.99	0.75	3 6	1 0	1 2	3765	57	126	0.07	0.06
					−3 −6	−1 0	−1 −2	3486	58	119		
54	85	120	5.14	0.73	4 6	1 0	0 1	2495	60	95	0.01	0.10
					−4 −6	−1 0	0 −1	2524	62	97		
55	88	120	5.22	0.47	4 6	0 1	1 1	691	33	38	0.09	0.29
					−4 −6	0 −1	−1 −1	750	33	39		
71	112	120	5.90	0.80	4 7	1 1	0 2	672	53	56	0.03	0.04
					−4 −7	−1 −1	0 −2	655	54	57		
78	125	120	6.22	0.52	5 7	1 1	1 1	1844	58	80	0.07	0.05
					−5 −7	−1 −1	−1 −1	1724	60	79		
78	125	120	6.22	0.52	−5 −7	−1 −1	−1 −1	1919	78	96	0.00	0.05
					5 7	1 1	1 1	1925	72	92		
83	132	120	6.40	0.72	4 8	0 1	1 1	1436	62	75	0.09	0.09
					−4 −8	0 −1	−1 −1	1560	61	76		
86	137	120	6.52	0.69	4 8	1 2	0 1	1366	61	73	0.11	0.04
					−4 −8	−1 −2	0 −1	1218	63	72		
92	148	120	6.77	0.44	5 8	1 1	0 1	9147	80	285	0.00	0.13
					−5 −8	−1 −1	0 −1	9170	80	286		
95	152	120	6.86	0.62	5 8	1 2	1 0	1693	53	73	0.01	0.17
					−5 −8	−1 −2	−1 0	1683	53	73		
95	152	120	6.86	0.62	5 8	1 0	1 2	947	47	54	0.00	0.17
					−5 −8	−1 0	−1 −2	946	48	55		
98	157	120	6.97	0.59	5 8	0 1	2 2	1839	55	77	0.01	0.07
					−5 −8	0 −1	−2 −2	1820	56	78		
118	189	120	7.65	0.66	5 9	1 1	1 3	1136	51	61	0.04	0.01
					−5 −9	−1 −1	−1 −3	1176	52	62		

Table 1. Continued.

N	M	Multiplicity	Q_{par}	Q_{perp}	h/h'	k/k'	l/l'	I_{norm}	$\sigma_{Poisson}$	σ_{tot}	DI/I	$(DI/I)_{calc.}$
124	200	120	7.86	0.38	6 9	1 2	1 1	20809	102	632	0.00	0.18
					−6 −9	−1 −2	−1 −1	20774	101	631		
131	211	120	8.08	0.46	6 9	0 1	2 3	2683	53	96	0.01	0.14
					−6 −9	0 −1	−2 −3	2643	54	95		
143	231	120	8.45	0.29	6 10	1 1	1 2	9111	73	282	0.01	0.08
					−6 −10	−1 −1	−1 −2	9027	72	280		
150	241	120	8.64	0.62	6 10	1 0	2 3	1190	46	58	0.00	0.04
					−6 −10	−1 0	−2 −3	1192	46	58		
176	284	120	9.37	0.42	7 11	0 1	1 2	3054	58	108	0.00	0.20
					−7 −11	0 −1	−1 −2	3062	58	108		
174	281	120	9.32	0.35	7 11	1 1	1 1	4055	62	136	0.01	0.15
					−7 −11	−1 −1	−1 −1	4005	61	134		
199	320	120	9.95	0.67	7 12	1 0	1 2	1087	49	58	0.15	0.15
					−7 −12	−1 0	−1 −2	925	50	57		
208	336	120	10.19	0.35	7 12	1 1	2 3	9877	84	307	0.06	0.24
					−7 −12	−1 −1	−2 −3	9241	88	290		

Table 2. The same as table 1 for reflections in a symmetry position for which icosahedral symmetry guarantees that the scattering amplitude must be real.

N	M	Multiplicity	Q_{par}	Q_{perp}	h/h'	k/k'	l/l'	I_{norm}	$\sigma_{Poisson}$	σ_{tot}	DI/I
51	80	60	4.99	0.75	3 6	1 2	1 0	599	36	40	0.25
					−3 −6	−1 −2	−1 0	452	38	40	
54	85	60	5.14	0.73	3 6	0 1	2 2	2422	48	87	0.04
					−3 −6	0 −1	−2 −2	2316	49	85	
71	112	60	5.90	0.80	3 7	0 0	2 3	1685	61	79	0.04
					−3 −7	0 0	−2 −3	1753	60	79	
72	116	12	5.99	0.33	4 6	0 0	2 4	76902	299	2326	0.03
					−4 −6	0 0	−2 −4	74602	301	2258	
70	113	60	5.91	0.24	4 7	0 0	1 2	170939	316	5137	0.02
					−4 −7	0 0	−1 −2	168040	322	5051	
83	132	60	6.40	0.72	5 7	2 2	0 1	2795	66	106	0.01
					−5 −7	−2 −2	0 −1	2812	67	107	
86	137	60	6.52	0.69	5 7	1 1	1 3	1380	51	65	0.13
					−5 −7	−1 −1	−1 −3	1203	53	64	
111	179	60	7.44	0.37	5 9	1 2	0 0	7291	71	229	0.01
					−5 −9	−1 −2	0 0	7211	71	227	
118	189	60	7.65	0.66	5 9	1 3	1 1	1956	54	79	0.01
					−5 −9	−1 −3	−1 −1	1981	54	80	
122	197	60	7.80	0.30	6 9	0 0	1 2	28886	128	875	0.00
					−6 −9	0 0	−1 −2	28978	128	878	
123	199	12	7.84	0.06	5 8	0 0	3 5	26671	118	808	0.02
					−5 −8	0 0	−3 −5	26146	118	793	
131	211	60	8.08	0.46	6 9	2 3	0 1	174	39	39	0.44
					−6 −9	−2 −3	0 −1	98	40	40	
150	241	60	8.64	0.62	7 10	0 1	0 0	788	45	50	0.09
					−7 −10	0 −1	0 0	861	44	51	
175	283	60	9.35	0.19	7 11	1 2	0 0	12765	88	392	0.02
					−7 −11	−1 −2	0 0	12497	88	385	
199	320	60	9.95	0.67	7 11	0 0	2 5	773	49	54	0.07
					−7 −11	0 0	−2 −5	721	48	52	
208	336	30	10.19	0.35	8 12	0 0	0 0	10227	84	318	0.01
					−8 −12	0 0	0 0	10168	87	317	
267	432	20	11.55	0.06	8 13	3 5	0 0	1279	50	63	0.01
					−8 −13	−3 −5	0 0	1295	49	62	

larger than experimental errors. This can be illustrated in two different ways. The average calculated relative intensity variation is equal to 0.12 whereas the measured value is 0.04. This is a significant difference. One can also look at reflections with an intensity greater than 3000 (those for which the Poissonian standard deviation is smaller than 0.02 so that these reflections are more meaningful). In all cases the calculated variation is much larger than the measured value: for instance the 124/200 reflection has a calculated variation equal to 0.18 and a measured value lower than 0.01. All these results show that the phase difference between the two sublattices Pd and Al–Mn is significantly smaller than 45°. A reasonable lowest limit for measurable intensity differences would correspond to a phase shift of about 15°.

The present experiment tests only the phase difference between Al–Mn and Pd sublattices. A previous contrast variation experiment had already shown that the Al–Pd and Mn sublattices also have a phase difference of 0 or π [17]. This was obtained by measuring neutron powder diffraction spectra on a sample with isomorphic substitution on the Mn sites. Because of the use of powder samples, these results are somewhat less accurate than the present data, but they also show a centrosymmetrical character.

One possible drawback of this study would be the presence of 180° twins in the sample. In this case, Bijvoet pairs will necessarily have the same intensity under all conditions, because each peak is actually the superposition of Bragg peaks from two crystallites. In particular, we have mentioned that a mosaic spread study has shown two coexisting domains in the sample, with 0.02° misorientation. There is actually no way to decide whether this misorientation is not 179.88° instead. However, it happens that one of the two domains is twice the other. Thus a rotation of the sample by 180° would not result in equivalent situations with respect to diffraction if both crystallites were acentric, but it is fair to say that 180° twins are quite difficult to observe in quasi-crystals and their existence in the present sample cannot be completely ruled out.

Finally, one may consider that these results strongly suggest that the icosahedral Al–Pd–Mn phase is centrosymmetrical or at least presents a weak non-centrosymmetric character, i.e. phases are close to 0 or π, within a 15° uncertainty range.

5. Conclusion

The centric character of the icosahedral phase has been checked by measuring Bijvoet pairs above the Pd edge . The measured intensities do not show strong variation for HKL and $-H-K-L$ reflections. The intensity variation calculated for a 45° phase difference from an atomic model is larger than the measured value. These results are also consistent with previous contrast variation experiments, which tested the Al–Pd versus Mn sublattices. This suggests that the non-centric character, if any, must be very weak in the icosahedral Al–Pd–Mn phase. Further experiments using a brighter beam are in progress.

Acknowledgments

We are grateful to R Collela and S Burkov for useful discussions. The SUNY X3 beam line at the National Synchrotron Light Source is supported by the US Department of Energy under grant DEFG0291ER45231.

References

[1] Duneau M and Katz A 1985 *Phys. Rev. Lett.* **54** 2688
[2] Kalugin P A, Kitaev A Y and Levitov L S 1985 *JETP Lett.* **41** 145
[3] Elser V 1985 *Phys. Rev.* B **32** 4892
[4] Bak P 1985 *Phys. Rev. Lett.* **54** 1517–19; 1986 *Scr. Metall.* **20** 1199
[5] Janssen T 1986 *Acta Crystallogr.* A **42** 261
[6] Gratias D, Cahn J W and Mozer B 1988 *Phys. Rev.* B **38** 1643
[7] Janot C and de Boissieu M 1991 *Quasicrystals: the State of the Art* ed D P DiVincenzo and P J Steinhardt (Singapore: World Scientific) p 57; Janot C 1992 *Quasicrystals: A Primer* (Oxford: Oxford University Press)
[8] de Boissieu M, Janot C and Dubois J M 1988 *Europhys. Lett.* 7 593
[9] Janot C, Pannetier J, Dubois J M and de Boissieu M 1989 *Phys. Rev. Lett.* **62** 450
[10] Janot C, de Boissieu M, Dubois J M and Pannetier J 1989 *J. Phys.: Condens. Matter* **1** 1029
[11] de Boissieu M, Janot C, Dubois J M, Audier M and Dubost B 1991 *J. Phys.: Condens. Matter* **3** 1
[12] Kalugin P A 1989 *Europhys. Lett.* **9** 545
[13] Katz A 1990 *Number Theory and Physics* ed J M Luck, P Moussa M, Waldschmidt and C Itzykson (Berlin: Springer) p 100
[14] Duneau M and Oguey C 1989 *J. Physique* **50** 135
[15] Yamamoto A 1990 *Quasicrystals* ed T Fujwara and T Ogawa (Berlin: Springer) p 57
[16] Cornier-Quiquandon M, Quivy M, Lefebvre S, Elkaim E, Heger G, Katz A and Gratias D 1991 *Phys. Rev.* B **44** 2071
[17] Boudard M, de Boissieu M, Janot C, Dubois J M and Dong C 1991 *Phil. Mag. Lett.* **64** 197
[18] Boudard M, de Boissieu M, Janot C, Heger C, Beeli C, Nissen H U, Vincent H, Ibberson R, Audier M and Dubois J M 1992 *J. Phys.: Condens. Matter* **4** 10 149
[19] Saito M, Tanaka M, Tsai A P, Inoue A and Masumoto T 1992 *Japan. J. Appl. Phys.* **31** L109
[20] Lee H, Collela R and Chapman L D 1993 *Acta Crystallogr.* at press
[21] Lee H 1993 *Thesis* Purdue University
Lee H, Collela R and de Boissieu M 1993 *Bull. Am. Phys. Soc.* **38** 625
[22] Cornier-Quiquandon M, Bellissent R, Calvayrac R, Cahn J W, Gratias D and Mozer B 1992 *J. Non-Cryst. Solids* **153–4** 10
[23] Janssen T 1986 *Acta Crystallogr.* A **42** 261
[24] Rokshar D S, Wright D C and Mermin N D 1988 *Phys. Rev.* B **37** 8145
[25] Levitov L S and Rhyner J 1988 *J. Physique* **49** 1835
[26] Tsai A P, Inoue A, Yokoyama Y and Masumoto T 1990 *Phil. Mag. Lett.* **61** 9
[27] Tsai A P, Inoue A, Yokoyama Y and Masumoto T 1990 *Mater. Trans. Japan Inst. Met.* **31** 98
[28] Cahn J W, Shechtman D and Gratias D 1986 *J. Mater. Res.* **1** 13
[29] Coppens P 1992 *Synchrotron Radiation Crystallography* (New York: Academic)
[30] de Boissieu M, Durand-Charre M, Bastie P, Carabelli A, Boudard M, Bessiere M, Lefebvre S, Janot C and Audier M 1992 *Phys. Mag. Lett.* **65** 147